The stress distribution on the boundary of crazes in polyethylene by the direct and semi-theoretical method

Xue-qin Wang* and Norman Brown†
Department of Materials Science and Engineering, Laboratory for Research on Structure of Matter, University of Pennsylvania, Philadelphia, PA 19104, USA

and Leif-Olof Fager
Department of Mechanical Engineering and Applied Mechanics, University of Pennsylvania, Philadelphia, PA 19104, USA
(Received 18 July 1988; accepted 30 August 1988)

The stress distribution was determined on the boundary of crazes in a homopolymer and copolymer of polyethylene. The direct method was based on the direct measurement of the strain distribution and the stress–strain curve of the matrix. The semi-theoretical method was that of Wang and Kramer where the displacement profile of the craze was measured and the stress was calculated by a linear theory of elasticity. The assumption of linear elasticity in the matrix produces higher values of the stress when compared to the results of the direct method and the shape of the stress distribution is somewhat different.

(Keywords: craze; polyethylene; fracture)

INTRODUCTION

When a material with a sharp notch is loaded, a zone of damage generally initiates from the notch unless the material is so brittle that only crack growth occurs. The zone of damage may be in the form of a shear band, a craze, or a combination of the two. The zone of damage is generally the precursor for crack growth. The stress distribution on the boundary of the zone of damage plays an important part in our understanding of the fracture process. Many investigations have been made of this stress distribution for zones of damage in the form of crazes, shear bonds or an array of voids. These investigations have ranged from the purely theoretical to the purely experimental.

One of the simplest theories is by Dugdale[1], who assumed that for a thin planar zone of damage the stress normal to the damaged zone is constant and equal to the yield point. The Dugdale theory assumes that the matrix was an elastic–plastic non-work-hardening solid and thus predicts the size and shape of the damaged zone. Brown and Ward[2] and Doll[3] measured the geometry of crazes in poly(methyl methacrylate) (PMMA) using an interferometric technique and found agreement with the Dugdale theory. Imai and Ward[4] found that the Dugdale theory did not predict their observations on crazes produced by fatigue in PMMA and they calculated a non-uniform stress distribution to fit their craze geometry.

Knight[5], Verheulpen-Heymans and Bauwens[6], Wilczynski *et al.*[7], Walton and Weitsman[8], Bevan[9], Warren[10] and Wilkinson and Vitek[11] used a purely theoretical approach based on a theoretical model of the structure of the damage zone and on the assumption that the matrix was linear elastic.

Wang and Kramer[12] used a semi-theoretical method to determine the stress distribution. Their experimental input was the displacement profile of the damage zone and their theoretical equation for calculating the stress distribution was based on representation of a crack by a continuous array of dislocations as originally proposed by Bilby and Eshelby[13]. Again it was assumed that the matrix was linear elastic.

Brown and Wang[14] introduced a new purely experimental method for directly measuring the strain distribution along the boundary of a craze. Then from the actual stress–strain curve of the matrix, the stress distribution was directly inferred. In this paper the results of the Brown–Wang[14] method are compared with the results of the Wang–Kramer[12] method for two types of crazes in polyethylene. We used the same basic equation as presented by Wang and Kramer, but only modified the procedure for evaluating the basic integral.

In these experiments the length of the crazes were about one-tenth the length of the notch. Thus the equation (21b) in the Wang–Kramer paper[12] as derived by Hart[15] for the semi-infinite crack case appears to be most appropriate for calculating the stress distribution, $S(x)$, where:

$$S(x)=\frac{E^*}{4\pi}\int_0^a \frac{\alpha(t)}{x-t}\left(\frac{x}{t}\right)^{1/2} \mathrm{d}t \qquad (1)$$

where $\alpha(x)=-2\partial w(x)/\partial x$ and $E^*=E$ for plane stress and $E/(1-\nu^2)$ for plane strain; E is Young's modulus and ν is Poisson's ratio; $w(x)$ is the displacement profile of the craze and is related to the measured thickness profile of

* Visiting scientist from the University of Science and Technology of China, Hefei, Anhui, People's Republic of China
† To whom correspondence should be addressed

0032-3861/89/030453-08$03.00

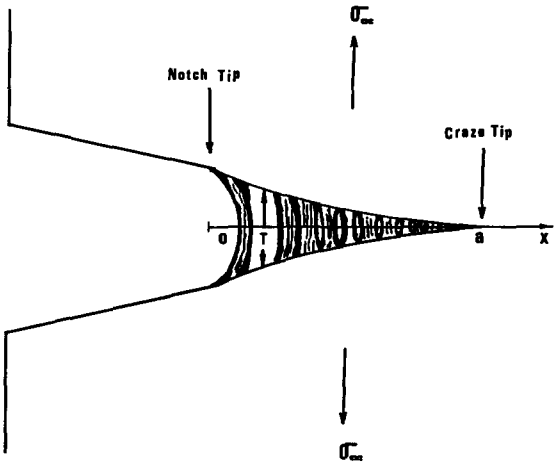

Figure 1 Schematic of craze

the craze, $T(x)$, by the equation:

$$w(x)=\tfrac{1}{2}T(x)[1-V_f(x)] \quad (2)$$

V_f is the volume fraction of the fibrils that constitute the craze and how it is measured will be described below. The length of craze is a, and x is the distance of a point from the origin at the notch tip (*Figure 1*). Since equation (1) involves a singularity wherever $x=t$, the integral in equation (1) cannot be evaluated by the common procedure. A detailed recipe for evaluating equation (1) is given in the Appendix. The details for determining $\alpha(x)$ by means of equation (2) will be given in the 'Experimental' section.

In applying equation (1) it is assumed that the zone of damage is thin in the sense that its aspect ratio is small. The length-to-thickness ratio of the crazes in this investigation is about 5. The crazes were produced in commercial resins of polyethylene under plane strain conditions and represent the same kind of crazes from which cracks slowly grow and which cause the type of field failures that occur in structural components.

Since the Wang–Kramer method is based on the assumption that the matrix is linear elastic and since polyethylene has a non-linear strain-softening type of stress–strain curve up to the yield point, the stresses from the Wang–Kramer method are generally greater than from the purely experimental method of Brown and Wang. It is the nature of equation (1) that the calculated stress at the tip of the craze is sensitive to the value of $\alpha(x)$, the gradient of the craze profile at the craze tip. Since $\alpha(x)$ is difficult to measure at the tip of the craze, the calculated stress at the notch tip is uncertain as pointed out by Wang and Kramer[12] and by Chudnovsky *et al.*[16].

It was found that the deformation surrounding a craze in polyethylene is more complex than the simple picture that the strain in the matrix is less than the yield strain. The actual contour of the tip of the notch not only affects the craze but also produces a concentration of strain at the sharp edges of the notch tip. These complex details were not reported in our previous paper[14], but now our confidence in the data has improved.

EXPERIMENTAL PROCEDURE

Materials

Two types of linear polyethylene (PE) were investigated: (1) a homopolymer (HPE), with $M_n=19\,600$ and $M_w=130\,000$; and (2) an ethylene–hexene copolymer (CPE) with 4.5 butyl chains per 1000 carbons, $M_n=15\,000$ and $M_w=170\,000$. The resins were compression moulded and very slowly cooled to room temperature. Notched specimens were exposed to a tensile stress for a given period of time. The craze that emanated from the notch was small compared to the dimensions of the specimen. The conditions of deformation were plane strain. An important difference between the two materials is that growth rate of the damage zone for the HPE is about 10^2 times faster than for the CPE[17]. Thus, the HPE is used for milk bottles and the CPE for gas pipes. The stress–strain curves for the two polymers are in *Figure 2*.

Measurement of the strain distribution

After a certain time, a specimen was unloaded and slices about 1–2 mm thick were taken from the centre of the specimen. The slicing was done with a fresh razor blade at a very slow controlled rate. The slice was then put in a small tensile jig (*Figure 3*) where, under a light microscope, the notch was opened by a definite amount relative to the original crack opening displacement (*COD*) that was observed prior to unloading the specimen for slicing. The slice was then coated with gold for the scanning electron microscope (SEM). SEM pictures are shown in *Figure 4*. Note the parallel scratches that were

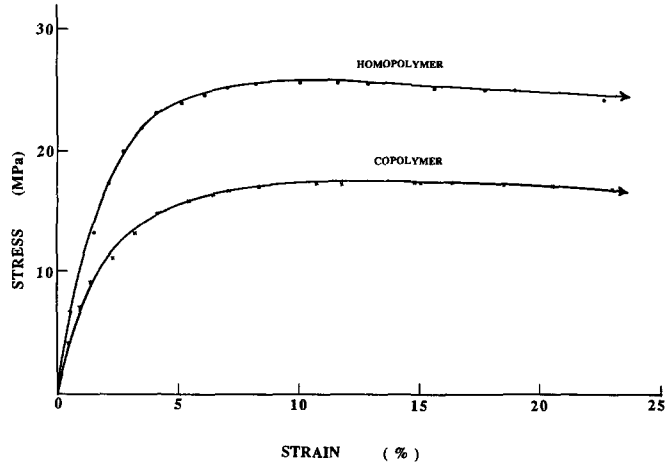

Figure 2 Stress–strain curve of homopolymer and copolymer at 26°C and strain rate 0.04 min^{-1}

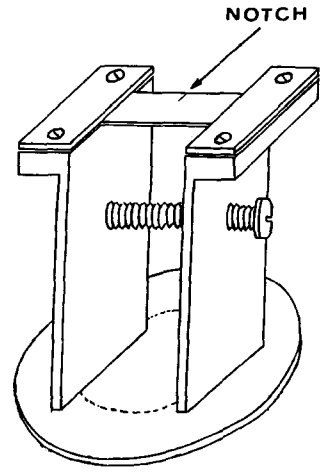

Figure 3 Tensile jig for SEM

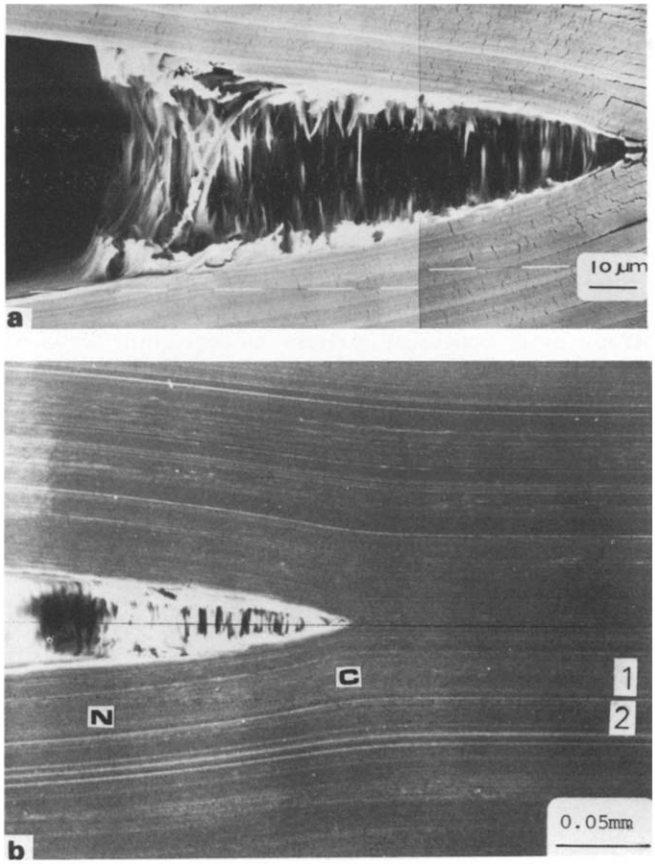

Figure 4 SEM micrographs of craze in homopolymer: (a) optimum contrast for observing fibrils; (b) optimum contrast for measuring strain. N is notch tip and C is craze tip (1 and 2 refer to strain positions in *Figure 6*)

produced by the razor blade when the specimen was sliced. Before loading the slice, the scratches were all parallel. After loading the slice, the spacing of the scratches changed by an amount that depended on the *COD*.

The SEM photograph was mounted on a wall and the spacing of the scratches was measured as a function of position by a low-power microscope with a filar eyepiece. Pairs of prominent scratches near the boundary whose spacing was about 0.02 mm apart were chosen for the measurements. The change in spacing of the pair of scratches could be measured with an accuracy of $\pm 0.5\%$. The reference point for zero strain was at a point near the boundary of the free surface of the notch where the stress is zero.

Measurement of the thickness profile

The boundary of the crazes, as shown in *Figures 4* and *11*, is irregular on a scale of 1 μm. The thickness of the craze profile was smoothed out by ignoring irregularities on the order of 1 μm. Particular difficulty was encountered at the craze tip which was not well defined. In order to avoid the calculated stress from becoming infinite at the craze tip, it was necessary to smooth the tip so that the gradient of the profile became zero at the craze tip. This localized smoothing at the craze tip is somewhat arbitrary and consequently the calculated stress very near the craze tip is highly uncertain. In order to minimize this uncertainty, the profile of scratches near the craze tip was used to determine the gradient in the region of the craze tip.

Measurement of the craze porosity

The method of measuring the craze porosity is based on the principle used by Lauterwasser and Kramer[18]. Instead of using the transmission electron microscope (TEM) to measure the relative densities of the crazed and uncrazed material, a method of micro-X radiography was used. A specimen about 1–2 mm thick was sliced with the razor blade and placed in a jig which kept the notch open during the exposure to the X-rays. A high resolution X-ray film (Kodak SO-343) was placed against the specimen which was exposed to unfiltered radiation from a copper anode under 45 kV voltage and a beam current of about 12 mA for about 10 min. The film was then optically enlarged 150 times in a Zeiss microscope (*Figure 5*). From the optical densities of the enlarged negative at the three locations (1) ϕ_n in the notch, (2) ϕ_c in the craze and (3) ϕ_m in the matrix, the porosity of the craze, $(1-V_f)$, can be calculated, where:

$$(1-V_f)=\frac{\ln(\phi_c/\phi_m)}{\ln(\phi_n/\phi_m)} \tag{3}$$

RESULTS

The craze in the homopolymer

Strain and stress by direct method. Figure 4a shows the SEM micrograph with the best contrast for observing the details of the fibrillar structure of the craze and the contour of the bottom of the notch. The sharp corners at the bottom of the notch were produced by the point of the razor blade. These points have been designated as the notch tip in *Figure 6*. Fracture of the fibrils at the base of the craze is evident. An SEM micrograph (*Figure 4b*) was taken so that the contrast of the scratches was enhanced. From *Figure 4b* the strain distribution was measured for two pairs of scratches 27 and 47 μm from the craze boundary (*Figure 6*). In *Figure 6* the strain distributions at 25 and 47 μm from the notch are similar. This fact indicates that the measured strain distribution is practically the same as the strain distribution closer to the boundary. Starting from a point in the matrix far from the craze tip, the strain is uniform and equal to 5.2% and 4.5% at distances of 27 and 47 μm respectively from the centre line of the craze. Thus, the far-field strain is about

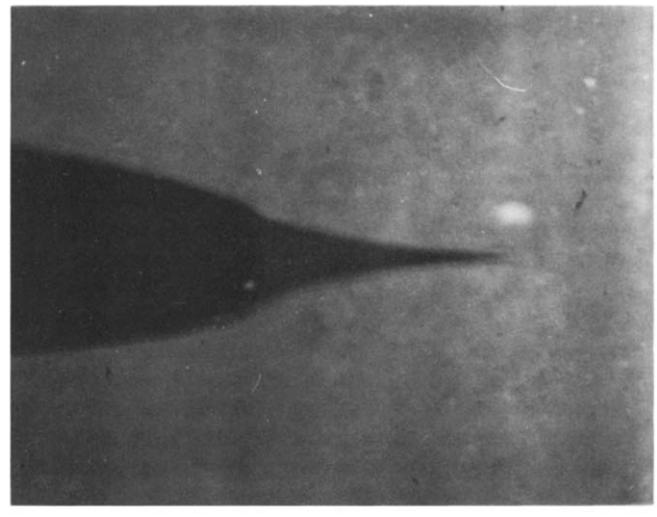

Figure 5 X-ray microradiograph of craze in copolymer

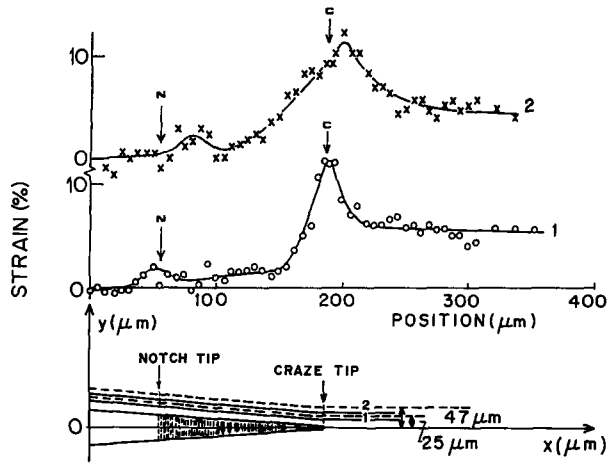

Figure 6 Strain distribution on boundary of craze in homopolymer

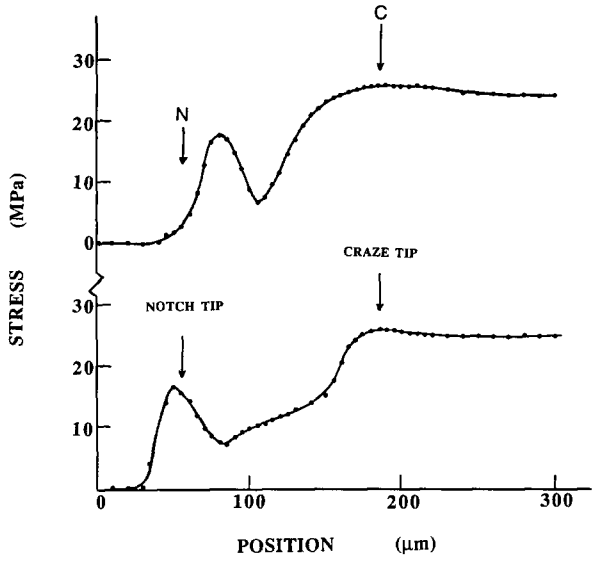

Figure 7 Stress distribution in homopolymer inferred from *Figures 6* and *2*

5%. A maximum in the strain of 11% occurs at the craze tip. From the craze tip towards the base of the craze the strain rapidly decreases to about 1%. In the vicinity of the notch tip the strain exhibits a secondary maximum of about 2.5% and then goes to zero beyond the notch tip. This secondary maximum is probably produced by the stress concentration produced by the sharp corner at the bottom of the notch. The fact that the strain becomes small in the neighbourhood of the base of the craze compared to the strain in the vicinity of the notch tip indicates that the fibrils near the craze tip are stronger than those near the base of the craze. This conclusion is supported by the micrograph of *Figure 4a* which shows a partial fracture of the fibrils in the vicinity of the base of craze.

The stress distribution (*Figure 7*) based on *Figure 6* was inferred from the stress–strain curve for the homopolymer in *Figure 2*. The stress in the matrix side of the craze tip appears to approach a value of 25 MPa. Since the depth of the notch, c, is 1000 μm and the stress in an elastic matrix is expected to decay approximately as $(c/x)^{1/2}$, then the value of the stress at 300 μm from the notch tip would not represent the far-field stress in an elastic solid. However since the matrix is a non-linear solid, as shown in *Figure 2*, it is expected that the stress would decay more rapidly than $(c/x)^{1/2}$. Probably 25 MPa represents the far-field stress in this specimen.

The maximum in the stress of 26 MPa at the craze tip is not as sharp as the corresponding maximum in the strain. The secondary maximum of 17 MPa in stress is more pronounced than the corresponding secondary maximum in strain. The secondary maximum in stress occurs very close to the notch tip for the point 25 μm away whereas this maximum occurs prior to the notch point for a point 47 μm away because the stress concentration tends to radiate from the sharp corner of the notch at an angle of about 45°. The shape of the stress distribution between the two maxima is different for the points 25 μm away compared to those 47 μm away from the boundary. Possibly this difference is associated with the interaction of the stress field from the crazed region with the stress field generated by the stress concentration at the sharp corner of the notch.

Calculated stress distribution. The stress was calculated with equation (1) based on the measurement of the thickness profile (*Figure 8*) for the craze in *Figure 4b*. The thickness profile determines $w(x)$ as given in equation (2) and with a value of $(1-V_f)\sim 0.5$ that was obtained from the X-ray micrograph. There were two problems in determining the profile of the craze. In the vicinity of the craze tip, not only was it difficult to determine the tip but the profile was not well defined at the tip. In order to avoid having an infinite stress at the notch tip, equation (1) requires that the gradient be zero at the craze tip. Thus, the dotted shape of the craze profile near the craze tip is somewhat arbitrary. The second problem was how to handle the undulation in the profile that was observed in the neighbourhood of the notch tip. The undulation is larger than the uncertainty in the measurement. One could smooth out the undulation as indicated by the continuous curve or one could use the actual data points. We decided to calculate the gradient for both cases. *Figure 9a* shows the gradient $\alpha(x)$ for the smooth profile and *Figure 9b* shows $\alpha(x)$ for the actual data points. The corresponding stress distributions from equation (1) are shown in *Figures 10a* and *10b*. The extreme sensitivity of the stress distribution to the differences in the gradient

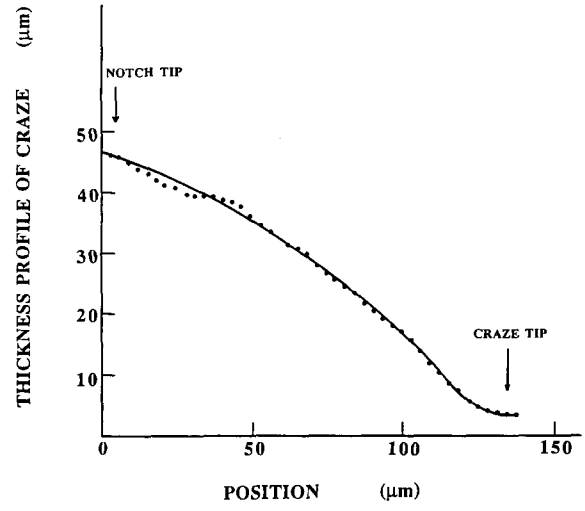

Figure 8 Thickness profile, $T(x)$, for craze in *Figure 4b*

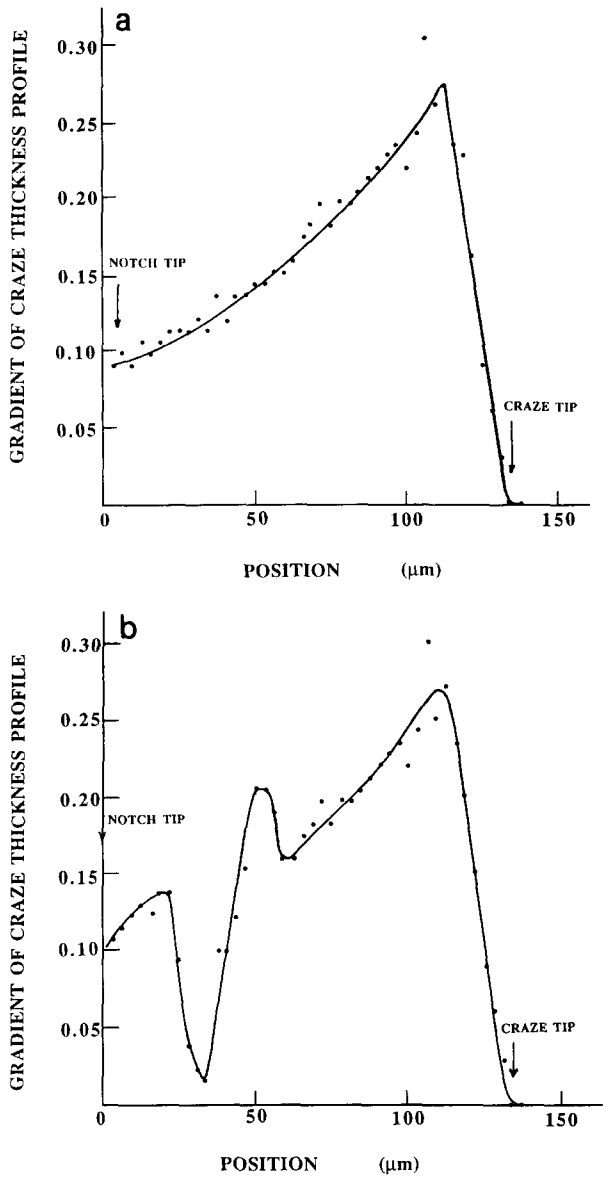

Figure 9 Gradient $\alpha(x)$ from *Figure 8*: (a) from smooth profile; (b) from actual data

distributions is very apparent. For this reason the stress distribution at the craze tip is very arbitrary since $T(x)$ is also somewhat arbitrary at the craze tip.

In calculating the stress distribution the plane stress value of $E^* = E$ was used because the craze profile was measured on a thin slice taken from the original specimen. However, the original craze was produced under plane strain conditions. The actual value of 1000 MPa for E was obtained directly from the homopolymer stress–strain curve in *Figure 2*. The choice of E is somewhat arbitrary because E depends on time. The strain rate for the stress–strain curve is different from the strain rate when the specimen was loaded in the tensile jig (*Figure 3*). In general the level of stress as calculated in *Figures 10a* and *10b* is higher than that by the direct method (*Figure 7*) because the calculated stress is based on the assumption of a linear elastic matrix. Both methods show a maximum at the craze tip. Both methods also give about the same value of 25 MPa for the asymptotic stress away from the craze tip.

The far field stress, σ_∞, was calculated as follows. The stress intensity was calculated from the equations[12]:

$$K = \frac{E^*}{2\sqrt{2\pi}} \int_0^a \frac{\alpha(t)}{t^{1/2}} \, dt \tag{4}$$

and

$$K = Y \sigma_\infty c^{1/2} \tag{5}$$

where Y is a geometry factor for the single edge-notched tensile specimen and has the value of $1.12\sqrt{\pi}$ for our specimen geometry according to Paris and Sih[19]; c is the length of the notch and equal to 2 mm. The results from equation (4) give $K = 1.0\,\text{MPa}\,\text{m}^{1/2}$, and the resulting value of σ_∞ is 12 MPa, which may be compared with the value of 25 MPa by the direct method.

The craze in the copolymer

Stress by direct method. Figure 11 is the SEM micrograph from which the strain distribution of *Figure 12* was measured. The point designated as the notch tip corresponds to the point where the tip of the razor blade produces the tip of the notch. During the original loading of the specimen the craze was produced and at the same time the rounded portion of the bottom of the notch between the base of the craze and the notch tip was produced. This rounded corner is a source of stress concentration which is probably the main cause of the maximum in the strain in its neighbourhood. The strain

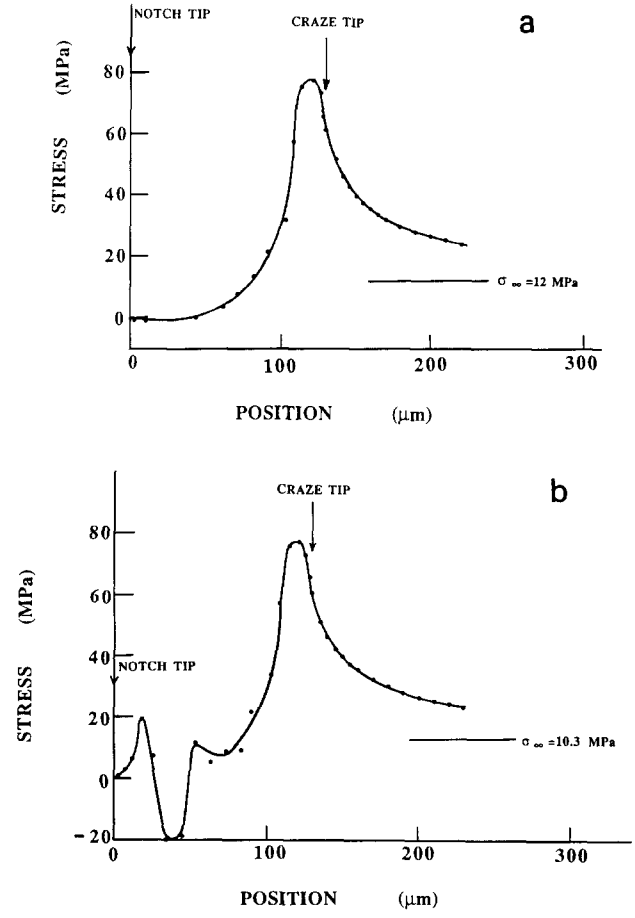

Figure 10 Stress distribution in homopolymer calculated with *Figure 9*: (a) from smooth profile; (b) from actual data

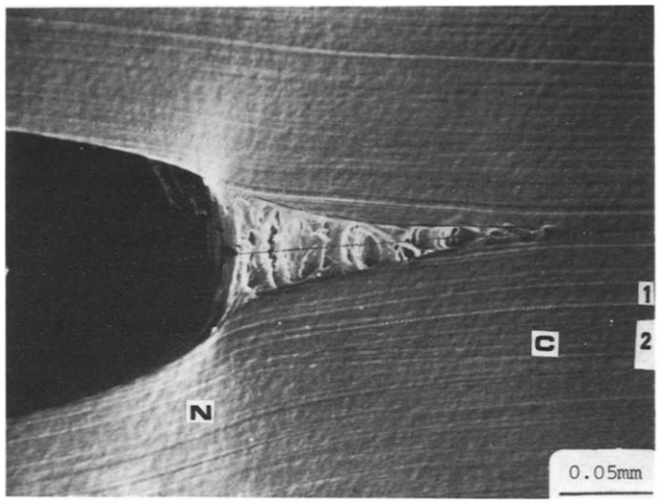

Figure 11 SEM micrograph of craze in copolymer. N is notch tip and C is craze tip (1 and 2 refer to strain positions in *Figure 12*)

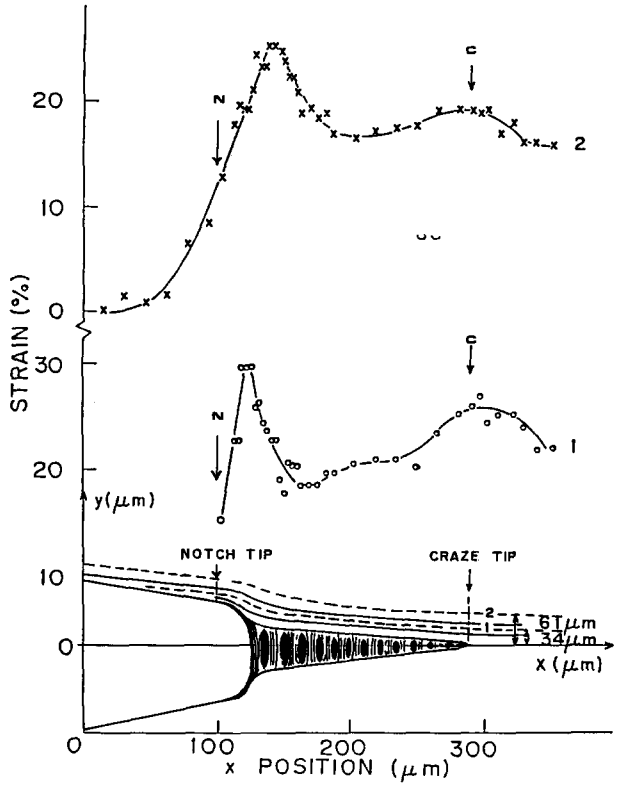

Figure 12 Strain distribution along boundary of craze in copolymer

field that emanates from the corners at the bottom of the notch are directly evident from the bright areas in the SEM micrograph in *Figure 11*.

Another maximum occurs at the craze tip. The strain distribution between the craze tip and the base of the craze is nearly constant at about 20%. In contrast to the homopolymer, where the strain rapidly decreased in going from the craze tip towards the base of the craze, the strain remains relatively high along the entire craze in the copolymer. This observation is consistent with the microscopic observation that no broken fibrils could be observed. Also the fibrils in the copolymer are generally much stronger than those in the homopolymer, as indicated by their high resistance to fracture by slow crack growth as shown by Lu, Wang and Brown[17].

As for the homopolymer, the strain distribution in the region near the base of the craze is somewhat more complex for the strain 34 μm from the boundary compared to that 61 μm from the boundary. Again it is suggested that this complexity is associated with the interaction between the strain produced by the fibrils and the strain produced by the stress concentration at the bottom of the notch.

The strains are appreciably larger than the yield strain, which is about 10%. The observed strains were produced when the crazed specimen was subsequently loaded in the tensile jig prior to being photographed in the SEM. Whereas the craze was originally produced with a crack opening displacement (*COD*) of 86 μm, the final *COD* was 103 μm.

The stress distribution in *Figure 13* was inferred from *Figure 12* and the stress–strain curve of the copolymer in *Figure 2*. The stress distribution is nearly constant between the craze tip and the notch tip. The stress distribution near the boundary of the notch is associated with the stress concentration at the notch tip and not with the fibrillar structure of the craze. The stress distribution curve A (*Figure 13*) stops at the surface of the notch because the corresponding scratches were terminated by the notch.

Calculated stress distribution. The thickness profile $w(x)$ of the craze in *Figure 11* is shown in *Figure 14*. The porosity $(1-V_f)$ was about 0.5. Since the craze boundary was not well defined at the craze tip, a pair of scratches near the craze tip were used to complete the profile. These measured points near the craze tip indicated that the gradient is finite at the tip. However, in order to avoid a singularity in the stress, the profile was smoothed out so that the gradient is zero at the craze tip. The corresponding gradient curve, $\alpha(x)$, is shown in *Figure 15* and the calculated stress distribution is in *Figure 16*. $E=700$ MPa was used as obtained from *Figure 2*.

In comparing the stress distribution by the direct method (*Figure 13*) against the calculated stress

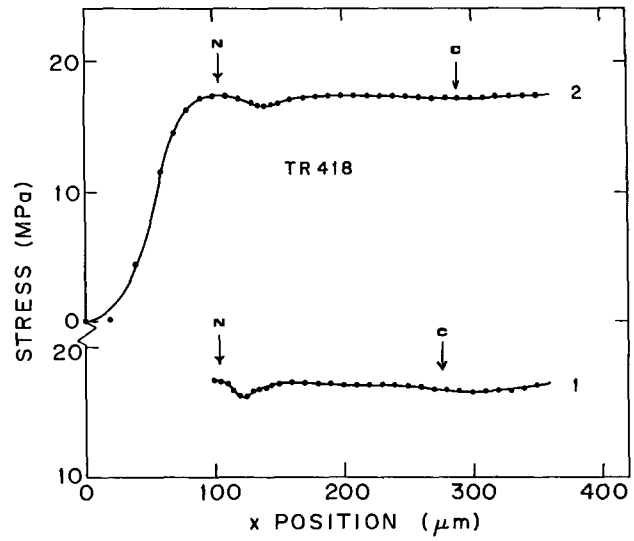

Figure 13 Stress distribution in copolymer inferred from *Figures 12* and *2*

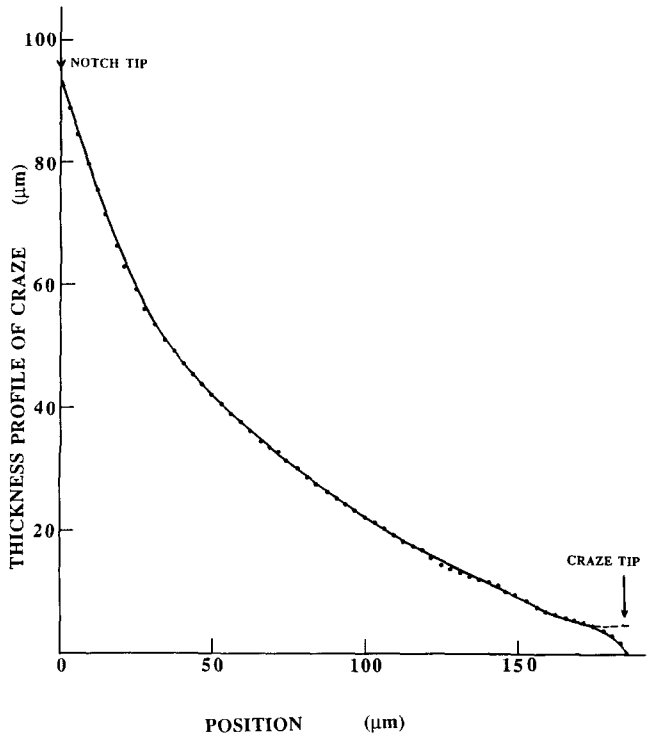

Figure 14 Thickness profile in copolymer, $w(x)$, for craze in *Figure 11*

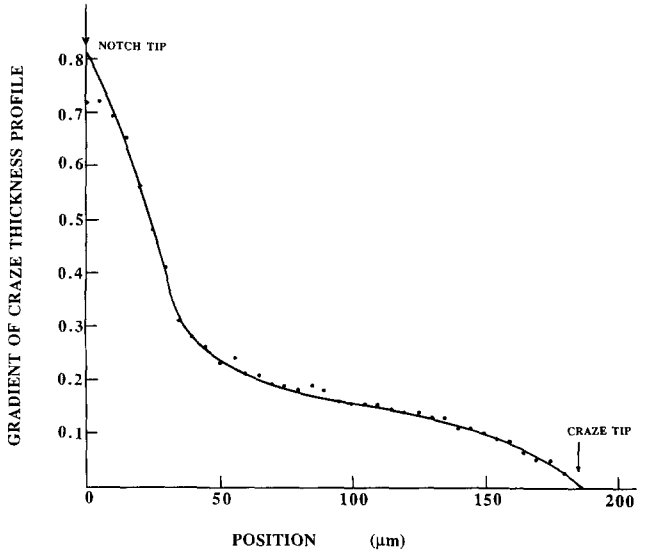

Figure 15 Gradient $\alpha(x)$ from *Figure 14*

distribution (*Figure 16*), both curves show a primary maximum at the notch tip. The general stress level is very much higher for the calculated stress and the asymptotic stress is twice that from the direct method. The calculated value of the asymptotic stress by means of equations (4) and (5) is 16.2 MPa, which compares very favourably with the value of 14 MPa by the direct method.

DISCUSSION

In general the calculated stresses are higher than those by the direct method as expected from the non-linear stress–strain behaviour of polyethylene. Also the calculated stress is unrealistic wherever it exceeds the yield point. A more linear elastic polymer such as polystyrene should give better agreement between the two methods.

The direct method is very useful in that it measures the total strain, both elastic and plastic. There are two sources of strain in the matrix: (1) the strain produced by the fibrils and (2) the strain produced by the stress concentrations from the sharp corners at the notch tip.

It is interesting to compare the homopolymer behaviour (*Figure 7*) with the copolymer (*Figure 13*). The decrease in stress in the homopolymer in going from the craze tip towards the notch indicates a gradual decrease in strength of the fibrils. The essentially constant stress between the craze tip and the notch in the copolymer indicates a uniformity in the fibril strength throughout the craze. Investigations of slow crack growth in these materials show that the fibrils in the copolymer tend to be much stronger than those in the homopolymer. However, the higher yield point of the homopolymer makes craze initiation more difficult in the homopolymer.

The direct method has several limitations. The inferred stress is not the same as the stress that existed at the time the craze was produced under plane strain conditions. In order to measure an appreciable amount of strain, the notch must be opened somewhat more than the amount of opening that existed at the time when the craze was produced. When the specimen is loaded in the jig to a fixed opening of the notch, the stress relaxes by an indefinite amount. Thus, the measured strain consists of a plastic, a creep and an elastic component, but the stress is determined only by the elastic component. In spite of these limitations the direct method is more closely related to the material behaviour than the semi-theoretical method. In future investigations the change in strain as a function of the amount of notch opening will be determined. In addition the change in strain distribution between the loaded and unloaded state will be presented. This change in strain should be most closely related to the stress distribution that existed prior to unloading since stress is related to the elastic component of the strain.

ACKNOWLEDGEMENTS

The Department of Energy and the Gas Research Institute sponsored the research. L.-O.F. was supported by the National Science Foundation. The Central Facilities of the Laboratory of Research on the Structure of Matter as supported by the National Science Foundation were most helpful.

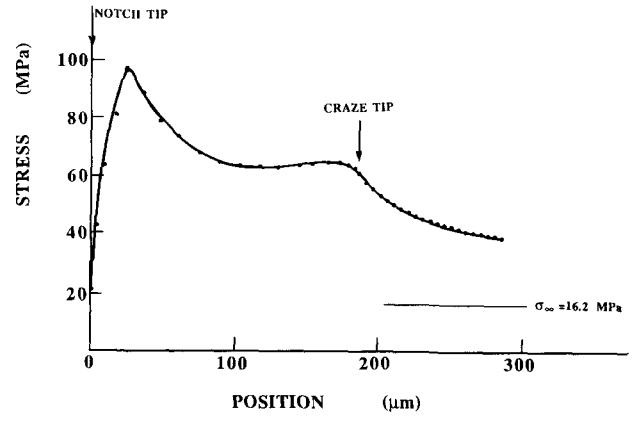

Figure 16 Stress distribution in copolymer calculated with *Figure 15*

APPENDIX

Method of evaluating equation (1)

For the case of semi-infinite crack loaded in mode I tension the stresses on the craze boundary can be calculated using the following equation given by Wang and Kramer[12]:

$$S(x)=\frac{E^*}{4\pi}\int_0^a\left(\frac{x}{t}\right)^{1/2}\frac{\alpha(t)}{x-t}\,dt \qquad (A1)$$

Note that this is a singular integral of Cauchy type and therefore the principal value must be evaluated. Following Erdogan *et al.*[20] a numerical integration procedure for singular integrals based on a quadrature formula of Gaussian type has been employed. After the customary transformation of the integration interval to $[-1,+1]$ equation (1) may be written:

$$S(\bar{x})=\frac{E^*}{4\pi}\int_{-1}^{1}V(\bar{t})\frac{(1+\bar{x})^{1/2}}{(1-\bar{t})^{1/2}}\frac{\alpha(\bar{t})}{\bar{x}-\bar{t}}\,d\bar{t} \qquad (A2)$$

where

$$V(\bar{t})=\frac{(1-\bar{t})^{1/2}}{(1+\bar{t})^{1/2}}, \qquad \bar{x}=\frac{2}{a}x-1 \qquad \bar{t}=\frac{2}{a}t-1$$

For this choice of $V(\bar{t})$ the right-hand side of (A2) can be evaluated at appropriately selected values $\bar{x}_k$ given by:

$$\bar{x}_k=\cos\left(\frac{2k-1}{2n+1}\pi\right), \qquad k=1,\ldots,n \qquad (A3)$$

The corresponding integration formula applied to (A2) yields:

$$S(\bar{x}_k)=\frac{E^*}{4\pi}\int_{-1}^{1}V(\bar{t})\frac{(1+\bar{x}_k)^{1/2}}{(1-\bar{t})^{1/2}}\frac{\alpha(\bar{t})}{\bar{x}_k-\bar{t}}\,d\bar{t} \qquad (A4)$$

$$=\frac{E^*}{4}\sum_{i=1}^{n}\frac{2}{2n+1}(1-\bar{t}_i)^{1/2}(1+\bar{x}_k)^{1/2}\frac{\alpha(\bar{t}_i)}{\bar{x}_k-\bar{t}_i}$$

where

$$\bar{t}_i=\cos\left(\frac{2i}{2n+1}\pi\right), \qquad i=1,\ldots,n$$

The choice of n will depend on the number of data points that are used to determine $\alpha(x)$.

REFERENCES

1 Dugdale, D. S. *J. Mech. Solids* 1960, **8**, 100
2 Brown, H. R. and Ward, I. M. *Polymer* 1973, **14**, 469
3 Doll, W. 'Crazing in Polymers', Advances in Polymer Science, Vol. 52/53 (Ed. H. H. Kausch), Springer-Verlag, New York, 1983
4 Imai, Y. and Ward, I. M. *J. Mater. Sci.* 1985, **20**, 3842
5 Knight, A. C. *J. Polym. Sci. (A)* 1965, **3**, 1845
6 Verheulpen-Heymans, N. and Bauwens, J. C. *J. Mater. Sci.* 1976, **11**, 1
7 Wilczynski, A. P., Liu, C. H. and Hsiao, C. C. *J. Appl. Phys.* 1977, **48**, 1149
8 Walton, J. R. and Weitsman, Y. *J. Appl. Mech.* 1984, **51**, 84
9 Bevan, L. *J. Polym. Sci., Polym. Phys. Edn.* 1981, **19**, 1759; *J. Appl. Polym. Sci.* 1982, **27**, 4263
10 Warren, W. E. *Polymer* 1984, **25**, 43
11 Wilkinson, D. S. and Vitek, V. *Acta Metall.* 1982, **30**, 1723; *J. Mech. Phys. Solids* 1975, **24**, 67
12 Wang, W.-C. V. and Kramer, E. J. *J. Mater. Sci.* 1982, **17**, 2013
13 Bilby, B. A. and Eshelby, J. D. 'Fracture' Vol. 1 (Ed. H. Liebowitz), Academic Press, New York, 1972, Ch. II, p. 111
14 Brown, N. and Wang, X. *Polymer* 1988, **29**, 463
15 Hart, E. W., private communication to Wang and Kramer 1980 in ref. 12
16 Chudnovsky, A., Mullen, R. and Warren, W. E. *Bull. Am. Phys. Soc.* 1984, **29** (3), KT2
17 Lu, X., Wang, X. and Brown, N. *J. Mater. Sci.* 1988, **23**, 643
18 Lauterwasser, B. D. and Kramer, E. J. *Phil. Mag. (A)* 1979, **39**, 469
19 Paris, P. C. and Sih, C. G. ASTM Technical Publication No. 381, American Society of Testing and Materials, Philadelphia, 1965, p. 30
20 Erdogan, F., Gupta, G. D. and Cook, T. S. 'Mechanics of Fracture' Vol. 1 'Methods of Analysis and Solutions of Crack Problems' (Ed. C. G. Sih), Noordhoff, Leyden, 1973, Ch. 7, p. 368